

HIGH COERCIVITIES IN HDDR PROCESSED Sm-Fe-Ta-N MAGNETS

VISOKE KOERCITIVNOSTI Sm-Fe-Ta-N MAGNETOV DOBLJENIH PO HDDR POSTOPKU

KRISTINA ŽUŽEK, P. J. MCGUINESS, S. KOBE

Institut Jožef Stefan, Jamova 39, 1001 Ljubljana, Slovenija

Prejem rokopisa - received: 1998-11-16; sprejem za objavo - accepted for publication: 1998-12-07

An alloy of composition $\text{Sm}_{13,8}\text{Fe}_{82,2}\text{Ta}_{4,0}$ was compared with a conventional $\text{Sm}_{13,7}\text{Fe}_{86,3}$ material in order to assess its potential as a permanent magnet material. The optimum conditions necessary to provide the highest coercivities using the HDDR process, and for the HDDR process combined with milling were investigated. The coercivities obtained after using the HDDR process and subsequent nitriding were 676,6 kA/m for the $\text{Sm}_{13,8}\text{Fe}_{82,2}\text{Ta}_{4,0}\text{N}_x$ and 358,2 kA/m for the $\text{Sm}_{13,8}\text{Fe}_{86,3}\text{N}_x$ samples. Coercivities of 1003,0 kA/m for $\text{Sm}_{13,8}\text{Fe}_{86,3}\text{N}_x$ and 1273,6 kA/m $\text{Sm}_{13,8}\text{Fe}_{82,2}\text{Ta}_{4,0}\text{N}_x$ were achieved by reducing the particle size with milling prior to the HDDR process. Magnetic results were compared with the phase composition, determined using scanning electron microscopy (SEM) and X-ray diffraction (XRD). The better coercivities obtained with the Ta containing sample were found to be due to the presence of a much smaller amount of αFe , a soft magnetic phase, with the TaFe_2 phase forming in its place. The milling prior to the HDDR treatment improves the magnetic properties because of the small particle size which prevents the grains growing too large, with their consequent very negative effect on the coercivity.

Key words: HDDR, SmFeN, Ta, coercivity, milling

Primerjali smo zlitino sestave $\text{Sm}_{13,8}\text{Fe}_{82,2}\text{Ta}_{4,0}$ z že poznano zlitino sestave $\text{Sm}_{13,8}\text{Fe}_{86,3}$. Želeli smo ovrednotiti potencial zlitine, z dodatkom Ta, z vidika permanentnega magnetnega materiala. Poiskali smo optimalne pogoje postopka HDDR, ki so nam dali najboljše rezultate na področju magnetnih lastnosti. Koercitivnosti prahov dobljenih po tem postopku in nadaljnem nitriranju, so 676,6 kA/m za $\text{Sm}_{13,8}\text{Fe}_{82,2}\text{Ta}_{4,0}\text{N}_x$ in 358,2 kA/m za $\text{Sm}_{13,8}\text{Fe}_{86,3}\text{N}_x$. Višje koercitivnosti 1003,0 kA/m za $\text{Sm}_{13,8}\text{Fe}_{86,3}\text{N}_x$ in 1273,6 kA/m za $\text{Sm}_{13,8}\text{Fe}_{82,2}\text{Ta}_{4,0}\text{N}_x$ pa smo dosegli z mletjem materiala pred HDDR postopkom. Rezultate magnetnih lastnosti smo primerjali tudi s fazno sestavo, ki smo jo določili z elektronsko vrstično mikroskopijo (SEM) in rentgensko difrakcijo (XRD). Razliko v višji koercitivnosti sestave s Ta, gre pripisati manjši vsebnosti αFe , ki kot mehkomagnetna faza znižuje magnetne lastnosti. αFe s tantalom tvori TaFe_2 fazo, ki pa je paramagnetna in nima negativnega vpliva na magnetne lastnosti. Tudi predmetlje materiala vpliva pozitivno na magnetne lastnosti saj z zmanjšanjem velikost delcev preprečimo grobo zrnatost, ki negativno vpliva na magnetne lastnosti.

Gljučne besede: HDDR, SmFeN, Ta, koercitivnost, mletje

1 INTRODUCTION

SmFeN magnets have received considerable attention since their discovery in 1991¹. Their intrinsic properties are comparable with, or better than, those of magnets based on $\text{Nd}_2\text{Fe}_{14}\text{B}$, and so they have the potential of taking a significant share of the rare earth permanent magnet market. SmFeN magnets are open to a number of possible processing routes, for example, mechanical alloying^{2,3}, melt spinning^{4,5} and conventional powder metallurgy^{1,6} however the HDDR process^{7,8} appears to be the most promising.

In this paper we have investigated the effects of a Ta addition on the magnetic properties and microstructure of a conventional SmFe cast alloy. Also the influence of milling, prior to the HDDR process, on the magnetic properties, will be discussed.

2 EXPERIMENTAL

The SmFe(A) and SmFeTa(B) cast alloys were produced by conventional induction melting methods in 5 kg batches by Less-Common Metals Ltd. The composition of the SmFeTa(B) alloy was chosen on the basis of our previous results^{9,10}. The ingot material was then

crushed to a particle size of less than 1 mm and the particle size reduced further by milling. Milling was carried out in an attritor mill for 30 minutes, under hexane in the inert atmosphere of a glove box. The HDDR processing was carried out in a rotating furnace operating between 1 bar over pressure and a vacuum of 10-2 mbar. The non pre-milled samples were introduced into the furnace as alloy lumps of less than 5 mm and the milled material as powder of approximately 5 μm particle size. The resulting non pre-milled HDDR powder was crushed by hand in a mortar and pestle to less than 200 μm . All samples were subsequently nitrided at 450°C for 4 hours in a flow of nitrogen gas. Permanent magnet bonded samples were produced by mixing the powder with epoxy resin, these samples were measured at room temperature in a conventional permeameter after pulsing the magnets in a field of 5 T.

3 RESULTS

The overall composition of the alloys is given in **Table 1**. Small pieces of approximately 0.5 cm³ were cut from similar parts of each alloy, mounted and polished for metallographic examination.

Table 1: Chemical composition of cast alloys**Tabela 1:** Kemijska sestava zlitin

	Sm (at%)	Fe (at%)	Ta (at%)
SmFe(A)	13.7	86.3	-
SmFeTa(B)	13.8	82.2	4.0

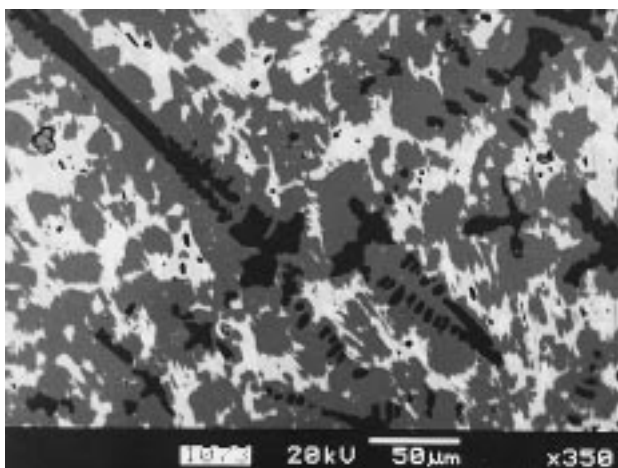
The resulting microstructures of the SmFe(A) and SmFeTa(B) materials in the as-cast condition can be seen in **Figure 1** and in **Figure 2**.

The conventional SmFe(A) (**Figure 1**) binary alloy exhibits the characteristic microstructure with dendrites of peritectically formed α -Fe, a $\text{Sm}_2\text{Fe}_{17}$ phase which forms the majority phase, with SmFe_2 and SmFe_3 observed to form at the grain boundaries. The results of the analysis confirm the existence of $\text{Sm}_2\text{Fe}_{17}$, SmFe_2 , SmFe_3 and α -Fe. The SmFeTa(B) alloy (**Figure 2**) is characterized by a very different microstructure. No α -Fe is observed. Rather, it appears that the primary phase in this case is TaFe_2 which forms throughout the alloy in grains of 1-10 μm . $\text{Sm}_2\text{Fe}_{17}$ is formed as the major phase and SmFe_2 and SmFe_3 are also observed to exist. The detected phases and their composition is given in a **Table 2**.

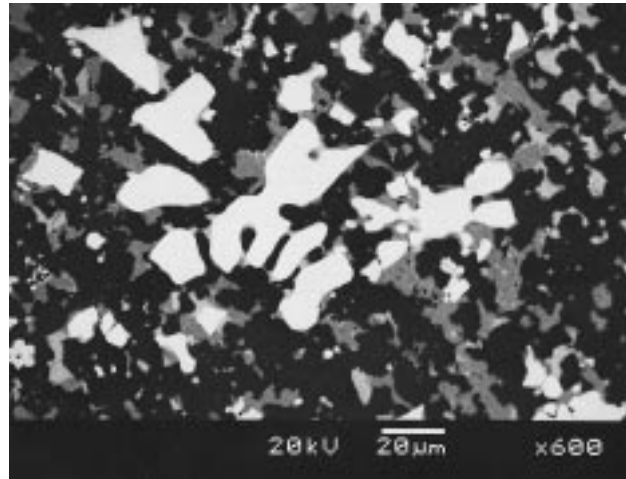
Table 2: Phases detected in both alloys, Sm-Fe(A) and Sm-Fe-Ta (B) and their composition**Tabela 2:** Detektirane faze v obeh zlitinah Sm-Fe (A) in Sm-Fe-Ta (B) in njihova sestava

SmFe (A)		SmFeTa (B)	
$\text{Sm}_2\text{Fe}_{17}$ phase	$\text{Sm}_{11}\text{Fe}_{89}$	$\text{Sm}_2\text{Fe}_{17}$ phase	$\text{Sm}_{10}\text{Fe}_{88}\text{Ta}_2$
SmFe_3 phase	$\text{Sm}_{25,2}\text{Fe}_{74,8}$	SmFe_3 phase	$\text{Sm}_{23}\text{Fe}_{75}\text{Ta}_2$
SmFe_2 phase	$\text{Sm}_{32,2}\text{Fe}_{67,8}$	SmFe_2 phase	$\text{Sm}_{30}\text{Fe}_{69}\text{Ta}_1$
αFe phase	$\text{Sm}_{0,1}\text{Fe}_{99,9}$	TaFe_2 phase	$\text{Ta}_7\text{Fe}_{30}$

In order to provide confirmation of the EDX data, XRD studies were undertaken on powdered samples of

**Figure 1:** SEM micrograph of the $\text{Sm}_2\text{Fe}_{17}$ cast alloy showing dendrites of primary Fe (dark), $\text{Sm}_2\text{Fe}_{17}$ (gray), SmFe_3 (light gray) and SmFe_2 (white) phases

Slika 1: SEM posnetek zlitine $\text{Sm}_2\text{Fe}_{17}$, ki prikazuje dendriško Fe fazo (črno), $\text{Sm}_2\text{Fe}_{17}$ fazo (sivo), SmFe_3 fazo (svetlo sivo), SmFe_2 (belo)

**Figure 2:** SEM micrograph of the Sm-Fe-Ta cast alloy with 4 at.% of Ta showing $\text{Sm}_2\text{Fe}_{17}$ (dark), SmFe_3 (gray), SmFe_2 (light gray), TaFe_2 (white) phases

Slika 2: SEM posnetek zlitine Sm-Fe-Ta s 4 at.% Ta, ki prikazuje $\text{Sm}_2\text{Fe}_{17}$ fazo (črno), SmFe_3 fazo (sivo), SmFe_2 fazo (sv. sivo) in TaFe_2 fazo (belo)

the cast SmFe(A) and SmFeTa(B) materials. **Figure 3** shows the two spectra obtained using Cu $K\alpha$ radiation. The lower spectrum from SmFe(A) shows clear evidence for the $\text{Sm}_2\text{Fe}_{17}$, SmFe_2 , SmFe_3 phases, as well as for α -Fe.

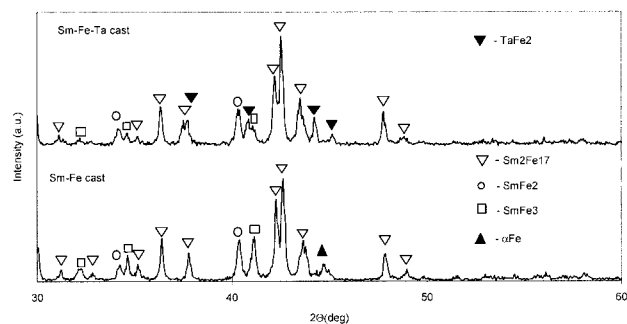
The upper spectrum, for the SmFeTa(B) material, again confirms the EDX results with the $\text{Sm}_2\text{Fe}_{17}$, SmFe_2 , SmFe_3 and TaFe_2 phases being detected.

In order to process materials with hard magnetic properties both samples, pre-milled and not pre-milled, SmFe(A) and SmFeTa(B) were HDDR processed according to the scheme in **Figure 4**.

3.1 Influence of Recombination Temperature on Coercivity

Non pre-milled material

Both types of samples exhibit peak coercivities at a recombination temperature of 750°C (**Figure 5**), but the SmFeTa(B) sample (676,6 kA/m) has almost twice the coercivity of the Ta free SmFe(A) binary alloy (358,2

**Figure 3:** X-Ray diffraction spectra of Sm-Fe (A) and Sm-Fe-Ta (B) cast alloys

Slika 3: Rentgenska difraktograma Sm-Fe (A) in Sm-Fe-Ta (B) zlitin

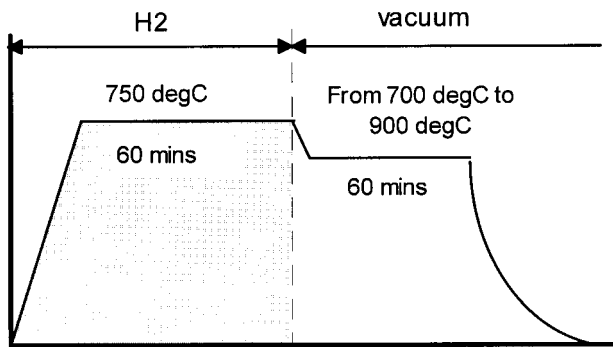


Figure 4: Heat treatment/atmosphere cycle for the HDDR process
Slika 4: Temperaturni profil in atmosferski pogoji pri HDDR procesu

kA/m). Because the Ta substantially reduces the presence of iron and its negative effect on the material's coercivity. The coercivity decreases at temperatures higher than 750°C because the recombined grains of 2:17 phase are too large.

Pre-milled material

The coercivity of SmFeN and SmFeTaN prepared by gas-solid reactions, can be increased by milling from 358,2 kA/m to 1003,0 kA/m for SmFeN and from 676,6 kA/m to 1273,6 kA/m for SmFeTaN (**Figure 5**). In comparison with non pre-milled samples the coercivity of pre-milled samples remains high above 750°C and in fact gets higher at temperatures between 780°C and 880°C. The small particle size (5 μm), prevents any explosive grain growth and its consequent negative effect on coercivity. At higher temperatures above 880°C it seems likely that the fine powders are beginning to partially sinter which offers the possibility of further grain growth.

3.2 SEM Study on HDDR Processed Materials

SEM pictures (**Figure 6 and Figure 7**), show not pre-milled and pre-milled samples after HDDR processing, the difference in the particle size is obvious. The

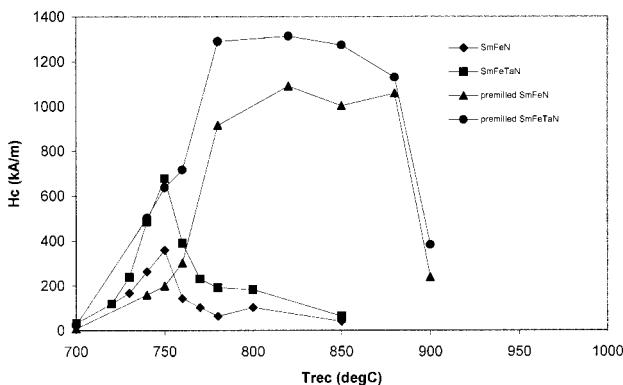


Figure 5: The coercivity force in dependence of recombination temperature for non pre-milled and pre-milled samples

Slika 5: Koercitivna sila v odvisnosti od temperature rekombinacije za mlete in nemlete vzorce pred HDDR procesom

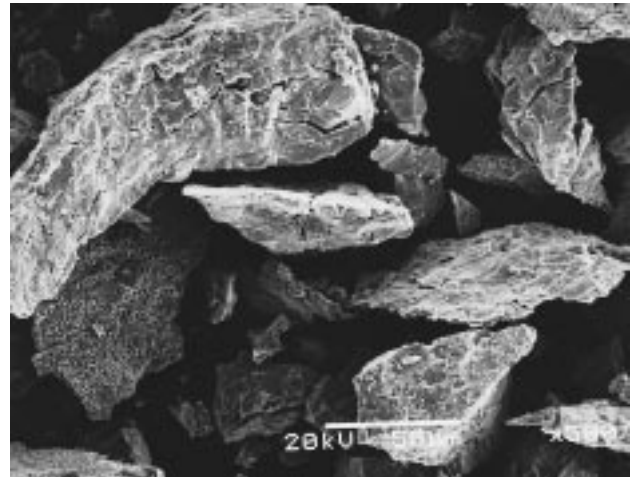


Figure 6: SEM micrograph of the non pre-milled SmFeTa sample after HDDR treatment ($T_{rec} = 850^{\circ}\text{C}$)

Slika 6: SEM posnetek ne mletega vzorca SmFeTa obdelanega po HDDR procesu ($T_{rek} = 850^{\circ}\text{C}$)

particle size of the non premilled material is about 100 μm (**Figure 6**), while the size of the pre-milled material, as was expected, is much smaller, about 5 μm (**Figure 7**). It has been observed that inside the particles (**Figure 6**) microcracks are found, which are the result of hydrogen absorption at the first stage of the HDDR process. This absorption results in a large volume expansion which causes the material to become friable or even to decrepitate.

The final step of the HDDR process is the recombination, when from Sm and αFe the Sm₂Fe₁₇ phase recrystallizes. These newly formed grains can be seen in the **Figures 8 and 9**. An interesting feature is the propensity of the recrystallized material to form idiomorphic grains (see **Figures 8 and 9**, indicated by arrow) which form by consuming the very fine initial grain

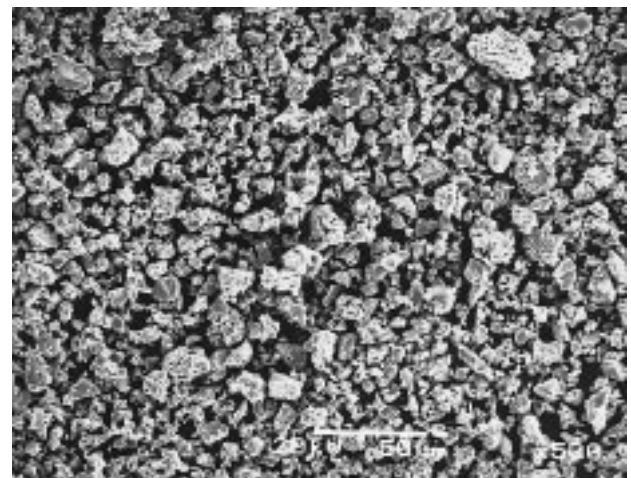


Figure 7: SEM micrograph of the SmFeTa sample after HDDR treatment ($T_{rec} = 850^{\circ}\text{C}$), pre-milled in attritor mill

Slika 7: SEM posnetek vzorca SmFeTa mletega v attritor mlinu in naknadno obdelanega po HDDR postopku

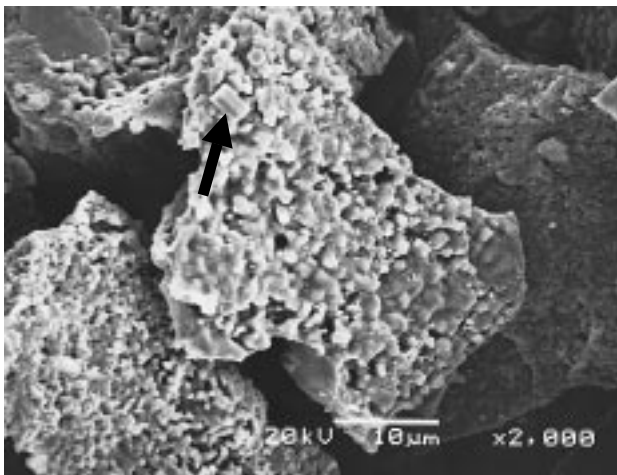


Figure 8: SEM micrograph of the non pre-milled SmFeTa sample after HDDR treatment ($T_{\text{rec}} = 850^{\circ}\text{C}$) showing the recrystallization of $\text{Sm}_2\text{Fe}_{17}$ phase of characteristic shape (indicated by arrow)

Slika 8: SEM posnetek vzorca SmFeTa, nemletega in obdelanega po HDDR postopku ($T_{\text{rek}} = 850^{\circ}\text{C}$), ki prikazuje proces rekristalizacije $\text{Sm}_2\text{Fe}_{17}$ faze, ki kristalizira v karakteristični obliki (označeno s puščico)

structure. Similar grain morphologies have been observed in NdFeB material¹¹.

4 CONCLUSIONS

The introduction of Ta has a very significant and beneficial impact on both the cast material and the final nitrated HDDR product. The enhanced values of coercivity indicate the critical importance of Ta in reducing as far as possible any free iron in the material.

The coercivity of the HDDR material strongly depends on the recombination conditions, which have to produce grains of an optimum size. Only the absence of the large grains can provide us with high coercivities.

Milling of the material before the HDDR treatment reduces the particle size and prevents the grains from growing to a size which influences negatively the coercivity. At elevated temperatures the coercivity drops because of sintering and agglomeration, which allows larger grains to form.

ACKNOWLEDGEMENT

The Ministry of Science and Technology of Slovenija is gratefully acknowledged for the provision of research funds.

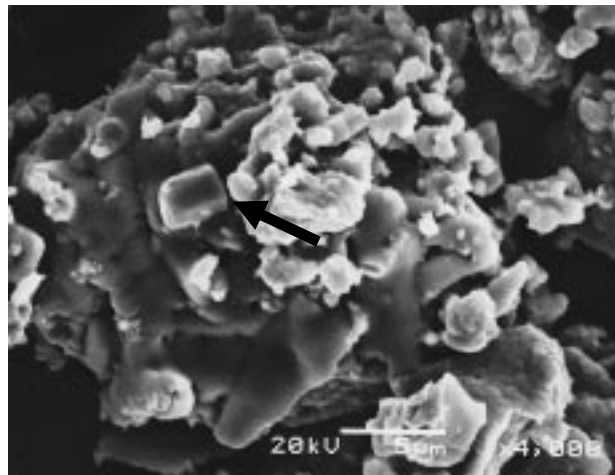


Figure 9: SEM micrograph of the SmFeTa sample after HDDR treatment ($T_{\text{rec}} = 850^{\circ}\text{C}$), pre-milled in attritor mill, showing the recrystallization of $\text{Sm}_2\text{Fe}_{17}$ phase of characteristic shape (indicated by arrow)

Slika 9: SEM posnetek vzorca SmFeTa mletega v attritor mlinu in naknadno obdelanega po HDDR postopku ($T_{\text{rek}} = 850^{\circ}\text{C}$), ki prikazuje proces rekristalizacije $\text{Sm}_2\text{Fe}_{17}$ faze, ki kristalizira v karakteristični obliki (označeno s puščico)

5 REFERENCES

- ¹ J. M. D. Coey and H. Sun, *J. Magn. Magn. Mater.*, 87 (1991) L251
- ² K. Schnitzke, L. Schultz, J. Wecker and M. Katter, *Appl. Phys. Lett.*, 57 (1990) 2853
- ³ M. Endoh, M. Iwata and M. Tokunaga, *J. Appl. Phys.*, 70 (1991) 6030
- ⁴ M. Katter, J. Wecker and L. Schultz, *J. Appl. Phys.*, 70 (1991) 3188
- ⁵ C. N. Christodoulou and T. Takeshita, *J. Alloys & Comp.*, 196 (1993) 161
- ⁶ M. Q. Huang, L. Y. Zhang, B. M. Ma, Y. Zbeng, J. M. Elbicki, W. E. Wallace and S. G. Sankar, *J. Appl. Phys.*, 70 (1991) 6027
- ⁷ T. Takeshita and R. Nakayama, *Proc. 11th Int. Workshop on RE Magnets & their Appl.*, (1991) 49
- ⁸ P. J. McGuinness, X. J. Zhang, H. Forsyth and I. R. Harris, *J. Less-Common Met.*, 162 (1990) 379
- ⁹ B. Saje, S. Kobe-Beseničar, Z. Samardžija, A. E. Platts, D. Kolar, I. R. Harris, *J. Magn. Magn. Mater.*, 146 (1995) L251-L255
- ¹⁰ B. Saje, B. Reinsch, S. Kobe-Beseničar, D. Kolar, I. R. Harris, *J. Magn. Magn. Mater.*, 157/158 (1996) 76-78
- ¹¹ I. R. Harris, P. J. McGuinness, *J. Less-Common Met.*, 172-174 (1991) 1273-1284